

Seismic background noise along the RISTRA array of broadband seismic stations extending from west Texas to southeast Utah

by Joseph Leon

Abstract An analysis of the seismic background noise (SBN) recorded by a temporary linear array of broadband seismographic stations belonging to the Rio Grande Rift Seismic Transect (RISTRA) experiment was done. Project RISTRA is a collaboration by research institutions which will study teleseismic data recorded by a linear array of seismic stations spanning the west Texas Great Plains, the middle Rio Grande Rift and the southern Colorado Plateau. Seismic background noise levels at each station is characterized by taking the mean of multiple power spectral densities (PSDs) of representative samples of the total SBN at a station over time. The stations' average PSD of the ambient noise is compared to the mean PSD of the seismic noise observed across the entire array, allowing inferences to be made regarding relative noise levels at RISTRA stations. Results show a high degree of variability in noise levels across the transect. This is due probably to the variability in site conditions. Relatively high noise levels in the 1.0 -10 Hz range are observed at all of the Great Plains sites as well as the Rio Grande Rift stations. Little variability is seen in the SBN across the array in the microseismic frequency range of 0.07 to 0.2 Hz. Overall, long-period (0.003 - 0.03 Hz) noise is greater on the two horizontal components than on the vertical components, although there is greater variability in long-period noise on the vertical-

component. The Great Plains stations show the least amount of variability in the long-period band.

Introduction

Seismic data are influenced in part by the signal to noise ratio (SNR) at the recording site. Characterizing the seismic background noise (SBN) at seismic recording stations allows inferences to be made about the quality of data from particular events. Studies have been done to quantify the SBN at sites around the world (Given, 1990; Gurrola *et al.*, 1990; Given & Fels, 1993; Peterson, 1993; Li *et al.*, 1994; Stutzmann *et al.*, 2000; Vila, 1998), as well as studies that have looked at the effects of particular noise sources on SBN (Rodgers *et al.*, 1987; Withers *et al.*, 1996; Young *et al.*, 1996). Such investigations into SBN have been done for permanent recording stations with considerable variations in seismometer vault design, for stations equipped with downhole sensors, and for temporary stations (like those that house PASSCAL instruments) which typically have sensors on the surface or buried at very shallow depths.

Monitoring the ambient noise conditions at a site is commonly used to determine the utility of data recorded at seismic stations (Given, 1990; Li *et al.*, 1994). Detectability of seismic events can be increased by maximizing the SNR at a recording station either by decreasing noise or by increasing signal strength (Young *et al.*, 1996). Consequently, when selecting locations for seismic stations, one wants to know where the quietest available sites are and how noise can be most effectively minimized at a given site (Young *et al.*, 1996). Many studies of the earth's internal structure can be improved by decreasing the noise level, and a good quantification and understanding of the seismic background noise is the first step in reducing the noise level on seismic data (Stutzmann *et al.*, 2000).

In addition to the SBN, a station's ability to faithfully record seismic events is affected by the noise and distortions within the recording system itself (Rogers *et al.*, 1987). System noise has been shown to contribute slightly to the background noise at sites investigated by Powell (1992) and by Rogers *et al.* (1987). They found that although some observed high frequency spikes may be due to unknown vibrations of the equipment or to intrinsic seismometer noise, system noise levels are typically well below other sources of noise. However system noise could be a concern at very quiet sites.

Signals from desirable events may be obscured by earth noise arising from both natural and cultural sources. Examples of such noise sources include microseisms, wind, human activity, temperature changes, and atmospheric pressure changes. In general the seismic noise field at a location is comprised of body waves, fundamental and higher mode surface waves, and random ground motions (Powell, 1992). The amount of earth noise encountered is strongly dependent upon conditions at the recording site (Powell, 1992). Noise can be a function of frequency, location and time, and is a manifestation of source distribution, propagation effects and receiver site conditions (Powell, 1992).

Cultural noise is an obvious concern at seismic recording stations. Powell (1992) found that the effect of car traffic is to raise spectral levels in the interval of 0.8 - 5.0 Hz (with no obvious peak) in shallow deployments of a meter or less. Stutzmann *et al.* (2000) made similar observations. Diurnal variations in SBN resulting from human activity patterns have been observed by Li *et al.* (1994) and by Stutzmann *et al.* (2000). Given (1990) observed time-of-day variations at four IRIS/IDA stations in Eurasia with noise levels during the work day ranging from 1.0 - 14 dB higher than night levels for frequencies above 1.0 Hz.

Seasonal variations in SBN associated with microseismic activity also have been documented. These effects are seen at varying degrees, depending on site conditions and on the distance a station is from a shore line (Stutzmann, 2000). It has been found that the microseismic peak, observable around 0.2 Hz, tends to have a higher amplitude and a shift towards lower frequencies in fall and winter than in spring and summer (Stutzmann *et al.*, 2000; Vila, 1998; Given, 1990; Rodgers *et al.*, 1987).

Below 0.1 Hz, noise levels are predominantly influenced by thermal and barometric changes (Given, 1990). Temperature fluctuations and tilt can cause an increase in horizontal noise at long periods (Given and Fels, 1993). Long-period noise also arises when changes in local atmospheric pressure produce ground motion. Such ground motions can be a source of long period noise on the vertical component (Stutzmann *et al.*, 2000). Vila (1998) noted a clear correlation between noise amplitude spectra and atmospheric pressure in the long periods. Stutzmann *et al.* (2000) attributed noise in the period band of 20 -100 seconds to atmospheric perturbations as well.

A strong correlation has been shown between wind speed and SBN levels (Vila, 1998; Withers *et al.*, 1996; Young *et al.*, 1996). The absence of objects that couple wind energy to the ground (such as trees and man-made structures) is an important consideration in selecting a quiet site. Young *et al.* (1996) report that wind-generated noise is broadband (15 - 60 Hz) and apparently nonlinear, increasing dramatically when a wind speed threshold is exceeded. At surface installations the minimum wind speeds at which the SBN appears to be influenced has been documented to be 3 - 4 m/s by Young *et al.* (1996), 3 m/s by Withers *et al.* (1996), and 4 - 5 m/s by Gurrola *et al.* (1990). It has been demonstrated that placing a seismometer at depth greatly reduces the wind effects. The greatest gains in wind noise reduction appear to be realized within the first 100 m (probably less than 10 meters) (Young *et al.*, 1996; Withers *et al.*, 1996).

This study analyzes the SBN in the frequency range of 0.001- 10 Hz, along an extensive temporary array of broadband seismic stations, in order to characterize the seismic noise environment. Characterization is accomplished by looking at amplitude spectra of samples from each component separated into day and night time periods, as well as by looking at the ratio of each station's spectra to the overall average of the array. A brief description of the research project is given first.

Rio Grande Rift Seismic Transect Experiment

The Rio Grande Rift Seismic Transect (RISTRA) experiment is a collaborative research project undertaken by the New Mexico Institute of Mining and Technology, New Mexico State University, the University of Texas at Austin, Dinè College (Shiprock, NM campus) and Los Alamos National Laboratory. Project RISTRA employs a passive-source array of seismic recording stations designed to collect teleseismic data. Station coordinates and elevations are listed in Table 1 of the appendix. The array became fully operational in November, 1999, although some stations began recording data as early as July, 1999 (see Table 3 of appendix for station installation/removal dates). The main line of the array consists of 54 stations, spaced ~18 km apart, equipped with three-component broadband seismometers on loan from the PASSCAL instrument center. Stations on the main line are named by using the abbreviation of the respective state in which they lie, followed by a number from 1 to 54. The numbering begins in the southeastern part of the transect at TX01 and continues sequentially toward the northwestern-most station, UT54. A second line made up of three stations (MB01, MB04(b) & MB05) lies parallel to the main line. The location of each station is shown in Figure 1. Half of the stations were removed in March 2001; the remaining half, in May 2001.

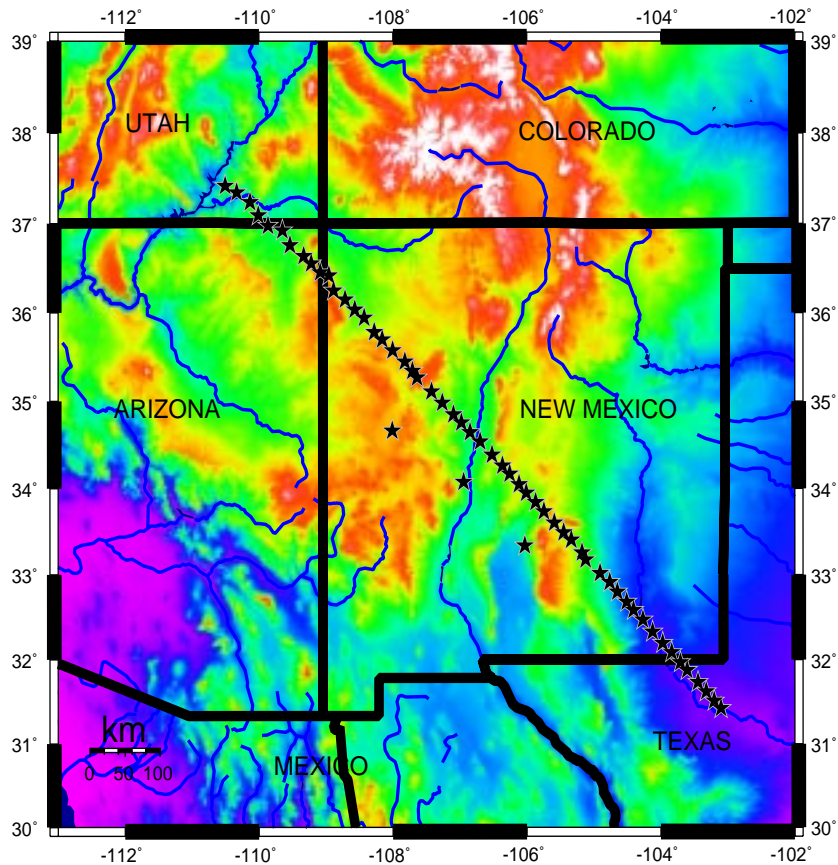


Figure 1. Locations of RISTRA stations are shown by stars. The three stations to the south-west of the main line are (from south-east to north-west) MB01, MB04(b), and MB05. Stations on the main line are numbered sequentially beginning in the south-east from 1-54. Color scale shows relative elevations.

The transect is oriented along a great circle path so as to optimize recording events from active regions with azimuths parallel to the line (Figure 2). These teleseismic data will (among other things) be used to produce a two-dimensional tomographic image of the subsurface along the array. Epicenters of some of the events recorded by the RISTRA array are shown in figure 2. The primary questions scientists from the participating institutions hope to address are: (1) what is the cause of the uplift of the Colorado Plateau; (2) to what depths do mantle processes that are con-

trolling surface tectonics extend; (3) what is the connection between mantle and crustal strain beneath the Rio Grande Rift region; and, (4) where in the mantle are the remnants of the Farallon plate and any possibly detached continental lithosphere.

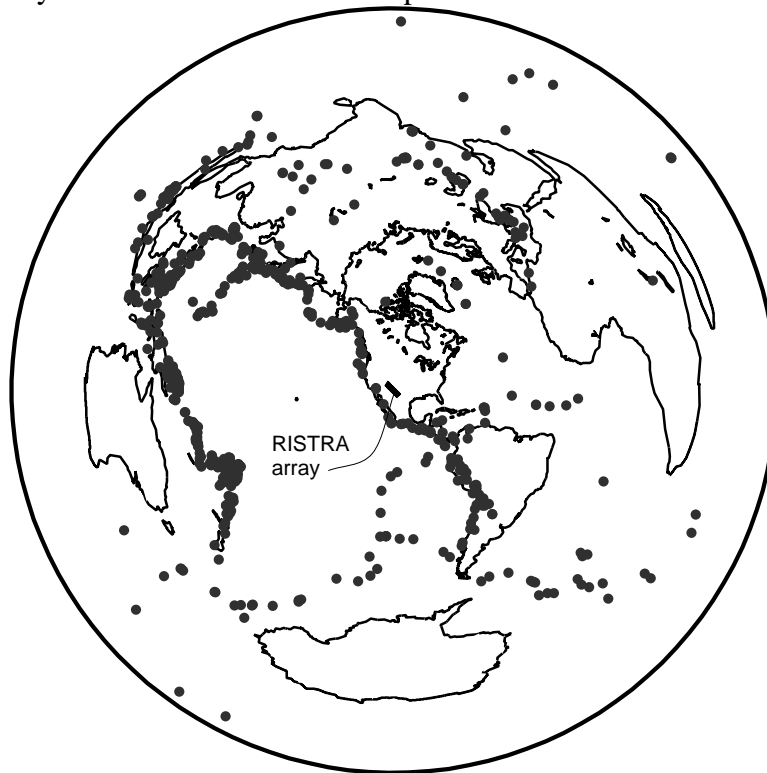


Figure 2. Orientation of the array relative to seismically active regions. Dots show events $M_b > 5.5$ recorded by the RISTRA array during the course of the deployment.

Instrumentation and Installation

All but one of the RISTRA stations are equipped with a Strekeisen STS-2 seismometer (standard response: 8.33 mHz (120 sec.) to 50 Hz). Station MB04(b) has a Guralp CMG-3T (standard response: flat velocity from 0.01 to 50 Hz). Both models are three-component sensors. Data are recorded at a rate of 20 samples per second and digitized using either a 24 bit, 72A-07 or 72A-08 RefTek data acquisition system.

In order to minimize thermally induced noise, by maintaining a constant temperature, the sensors are placed about 2 feet below the surface on a concrete pad, in either an insulated plywood vault or a styrofoam vault. About 2 feet of dirt is mounded on top of the vaults to further insulate them (Fig. 3).

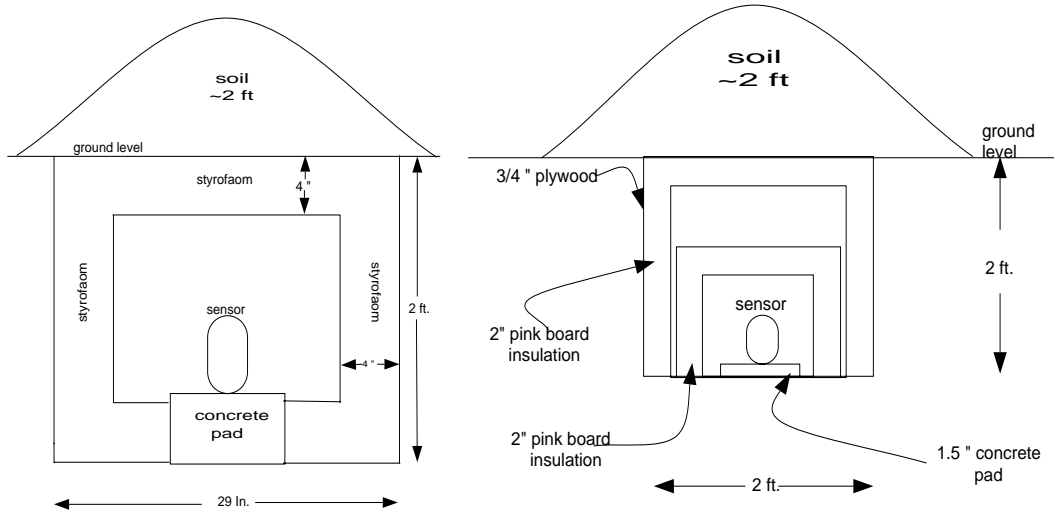


Figure 3. Two vault designs used in the RISTRA array.

The array spans a range of geologic as well as topographic and vegetation settings. Some sites are fairly remote and isolated from potential noise sources, others are near such cultural activities as rail and road traffic, gas and oil drilling and transportation, ranching, and agriculture. Table 2 (appendix) summarizes the site conditions and local potential noise source concerns for each station. Figure 4 depicts the large scale geological setting of the array.

Noise Analysis

An average power spectral density (PSD) of the background noise was calculated for each RISTRA station. "Quiet" (night time, between 2300 -0200 local time) and "noisy" periods (day time, from 1100-1400 local time) were sampled from each month of data collected between August, 1999 and November, 2000. Preliminary determination of epicenters reported by the NEIC were referred to in selecting each sample according to the following criteria: (1) no earthquake with Mb

≥ 6.0 is reported in the past 24 hours; (2) no earthquake with $M_b \geq 5.0$ reported from a distance < 70 degrees from the array in the past day; (3) no earthquake with $M_b \geq 4.0$ reported < 20 degrees away from the array in the previous 12 hours; (4) no earthquake with $M_b \geq 3.0$ reported < 15 degrees away from the array in the previous 3 hours. Samples were visually inspected to ensure that earthquake events had been excluded. Electronic spikes and glitches were removed by cutting them out of the samples when present.

An attempt was made to sample at least three hours of "quiet" time and three hours of "noisy" time from each month per station during the sampling period. Due to two different data retrieval methods the noise samples were obtained as files of either 3-hour or one-hour time series. The one-hour files are taken consecutively from the same three hour "noisy" and "quiet" periods as the three-hour samples (there are just three one-hour files sampling the same time period as one three-hour sample). The sample files from August, 1999 through July, 2000 are 3 hours in length. Files from August, 2000 through November, 2000 are one hour long each, but still cumulatively achieve the same sampling frequency as the three-hour samples.

Noise conditions at each RISTRA station are characterized by taking the mean of the PSD's of all data samples collected from each station and comparing them to an array average. Average station noise levels are determined by taking the mean of the PSD's from both day and night time samples combined. Separate day ("noisy") time and night ("quiet") time averages also were calculated. A mean background noise PSD for the entire array was calculated from individual station averages. Ratios of station mean spectra to the array mean spectra as a function of frequency were calculated for each station.

The number of sample files used in calculating the average PSD of each station's SBN is shown in figure A1 (appendix). The variability in the number of files used per station results from

the amount of data that met the criteria caused by station down time and other equipment problems -- and because files of two different lengths were used.

Power spectral densities of each sample noise file (having been converted to acceleration seismograms) were calculated by taking the FFT, with a Hahn taper over windows of 375 seconds (7500 sample), with 50% overlap. Spectra are shown in units of $\text{m}^2 / \text{s}^4 / \text{Hz}$.

Results

Plots of each station's average SBN spectrum are contained in Figure A2 of the appendix. The three components are shown individually along with Peterson's (1993) low and high noise models. Figure 5 displays the average background noise PSD over the entire array.

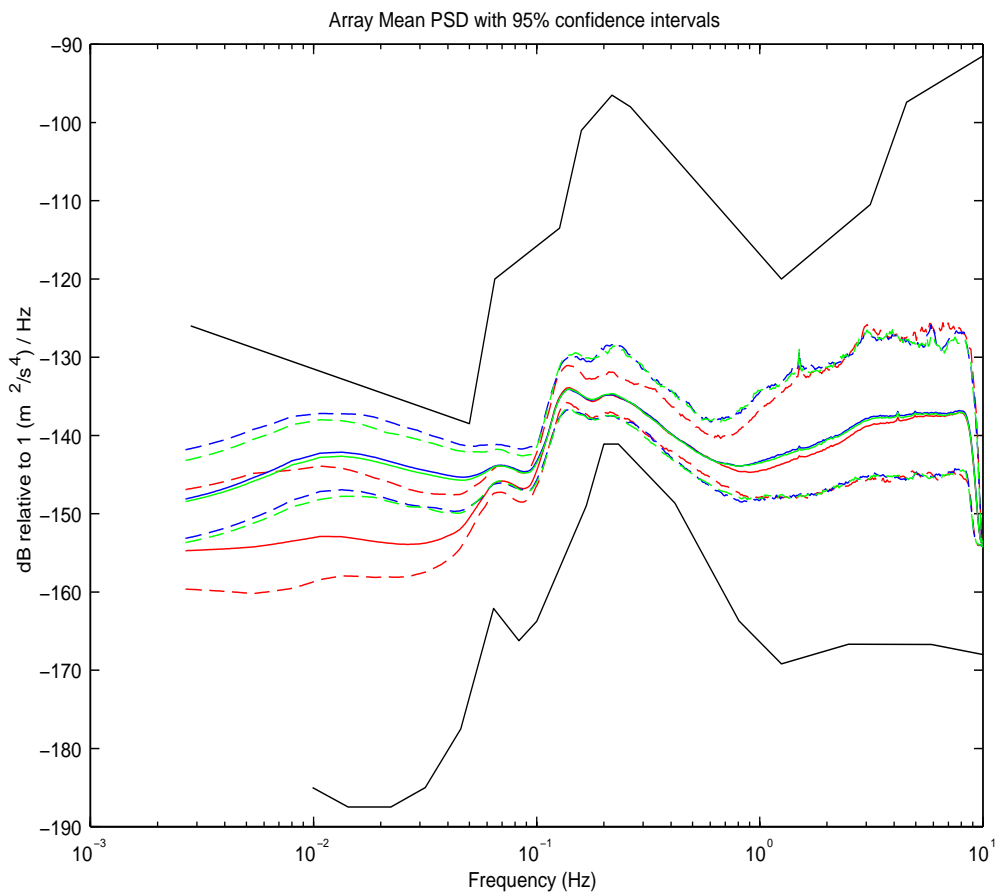


Figure 5. Mean PSD of entire RISTRA array. Each component is shown with its respective 95% confidence interval. Z-component is red, north-component is blue, east-component is green. Peterson's (1993) low and high noise models are in black.

Array-wide day and night time mean spectral levels are plotted for each of the three components in figure 6.

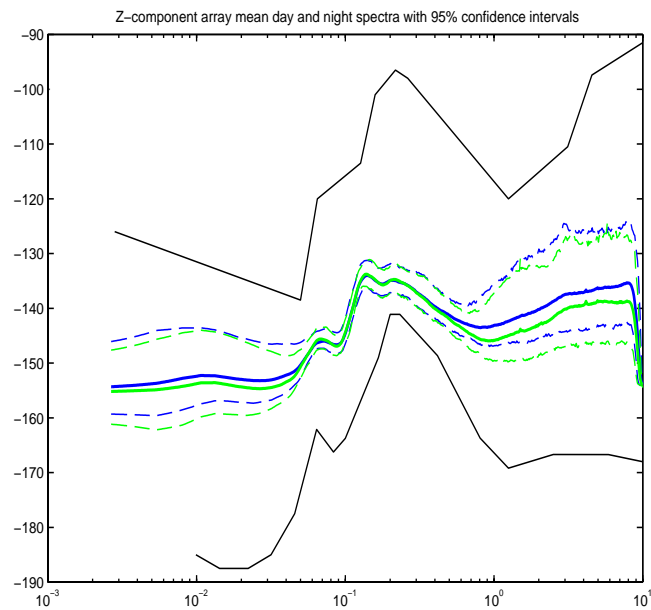


Figure 6 (a). Mean day and night time Z-component SBN PSD's for the entire array. Day time is in blue. Night time is in green. Peterson's (1993) low and high noise models are in black. Horizontal axis is frequency (Hz). Vertical axis is dB relative to $1 \text{ m}^2/\text{sec}^4/\text{Hz}$.

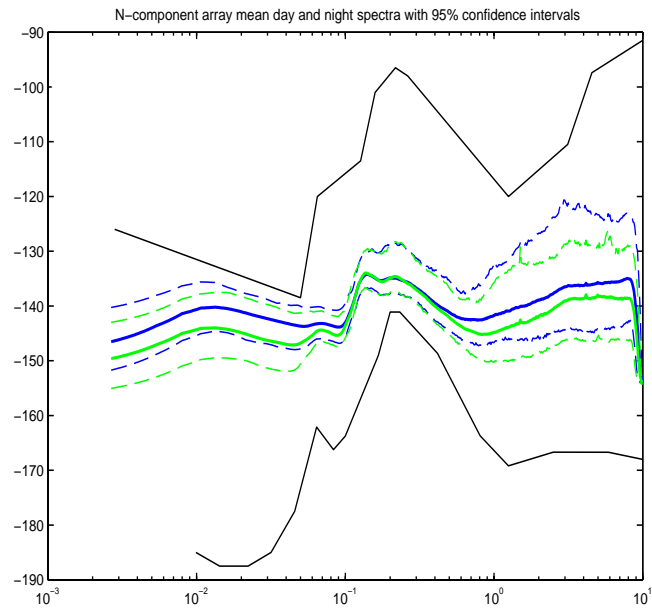


Figure 6 (b). Mean day and night time north-component SBN PSD's for the entire array. Day time is in blue. Night time is in green. Peterson's (1993) low and high noise models are in black. Horizontal axis is frequency (Hz). Vertical axis is dB relative to $1 \text{ m}^2/\text{sec}^4/\text{Hz}$.

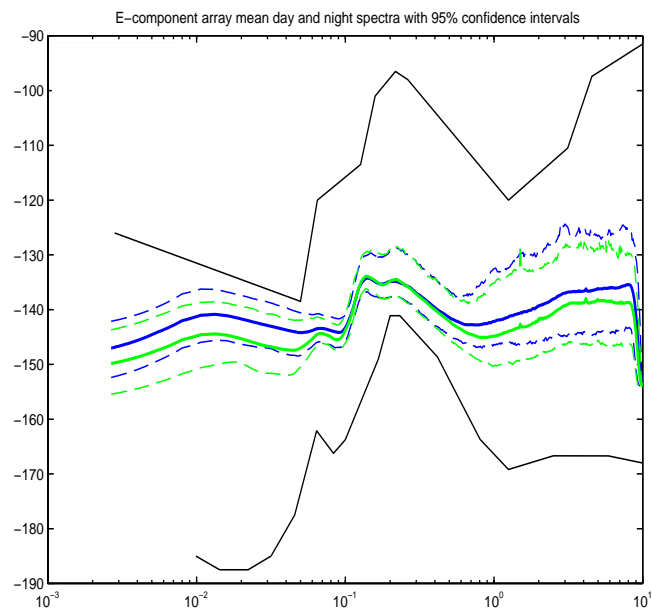


Figure 6 (c). Mean day and night time north-component SBN PSD's for the entire array. Day time is in blue. Night time is in green. Peterson's (1993) low and high noise models are in black. Horizontal axis is frequency (Hz). Vertical axis is dB relative to $1 \text{ m}^2/\text{sec}^4/\text{Hz}$.

Surface plots of the ratios of the mean spectra for each station to the mean spectra for the array as a function of frequency are given in figure 7 in which a single bar (or column) on the graph represents the plot of the station mean PSD / array mean PSD ratio vs. frequency of the respective station. The color scale is logarithmic, thus a ratio around 1.0 indicates a mean station noise level close to the array average. Noise levels greater than the array mean show up as peaks of yellow and red. Darker blues (ratio < 1.0) indicate frequencies at which the stations' noise levels are below the array mean.

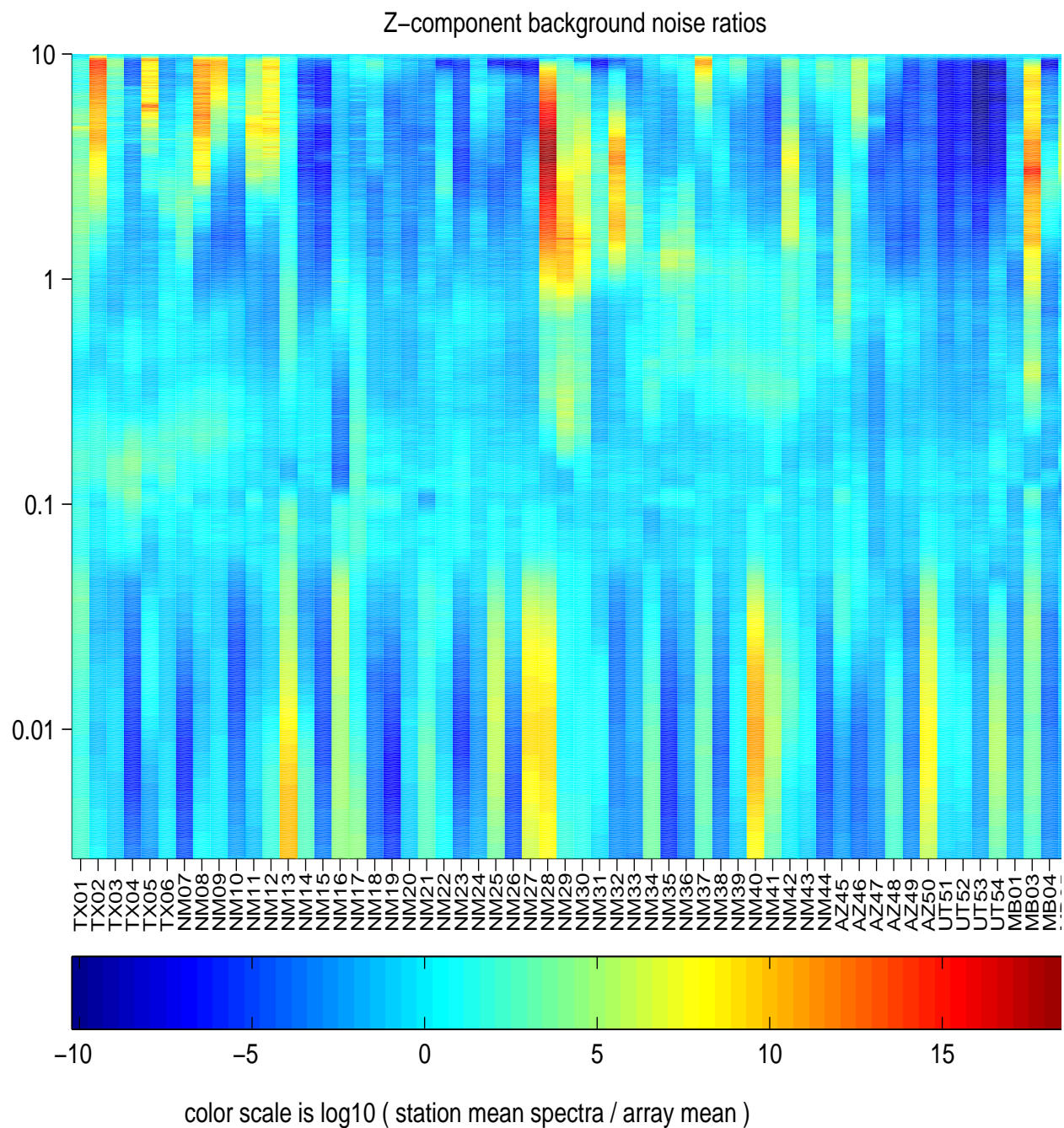


Figure 7 (a). Surface plot of the stations' vertical-component mean background noise spectra shown as a function of frequency. Note the frequency and the color bar are log scale. TX01-NM13 are the Plains stations, NM27-NM33 are the Rift stations. NM37-UT54 are the Plateau stations. The MB stations are the offline stations. Note station MB03 in the figure is actually MB04; MB04 on the figure is actually station MB04b. Vertical axis is frequency (Hz).

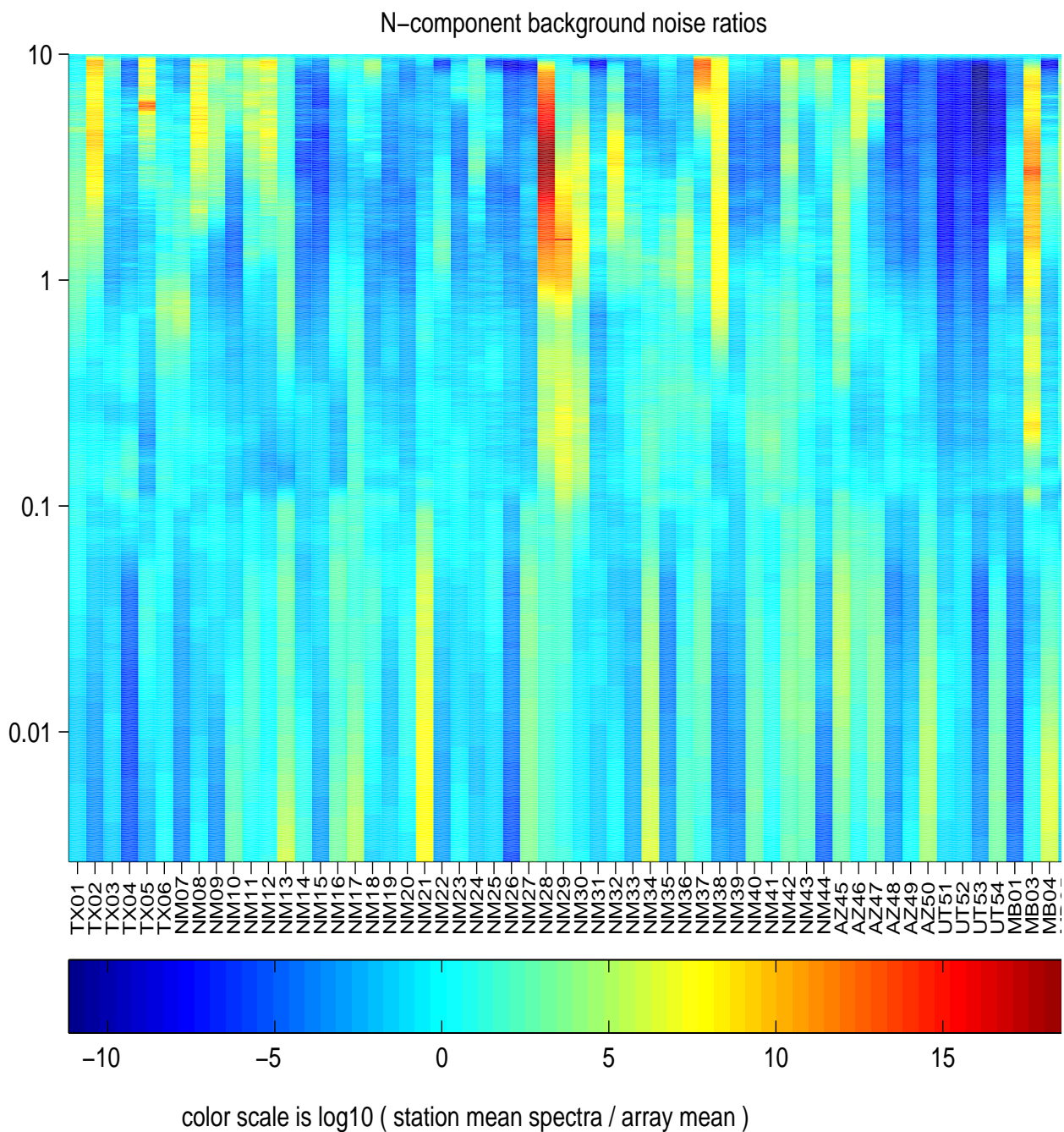
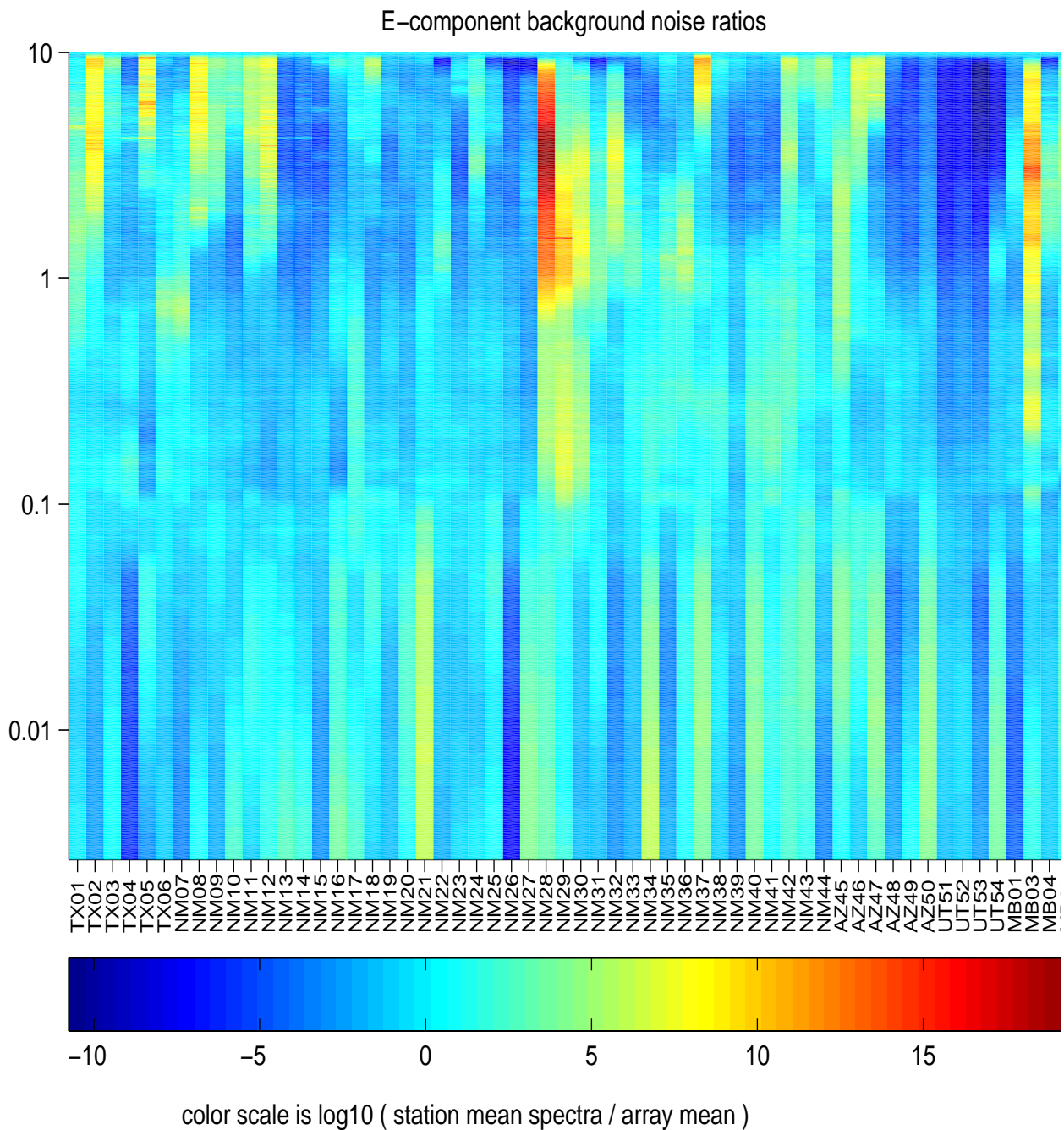


Figure 7 (b). Surface plot of the stations' north-component mean background noise spectra shown as a function of frequency. Note the frequency and the color bar are log scale. TX01-NM13 are the Plains stations, NM27-NM33 are the Rift stations. NM37-UT54 are the Plateau stations. The MB stations are the offline stations. Note station MB03 in the figure is actually MB04; MB04 on the figure is actually station MB04b. Vertical axis is frequency (Hz).



.Figure 7 (c). Surface plot of the stations' north-component mean background noise spectra shown as a function of frequency. Note the frequency and the color bar are log scale. TX01-NM13 are the Plains stations, NM27-NM33 are the Rift stations. NM37-UT54 are the Plateau stations. The MB stations are the offline stations. Note station MB03 in the figure is actually MB04; MB04 on the figure is actually station MB04b. Vertical axis is frequency (Hz).

A generalized geologic cross-section showing known geologic features as well as the stations' proximity to urban areas is provided in figure 8.

Discussion

The results reveal a large amount of variability in the SBN levels on the data recorded by the RISTRA array. The greatest variability is seen in the higher frequencies (1.0 -10 Hz), followed by the longer periods (0.003 -.03 Hz). The least amount of variation is seen in the 0.07 - 0.2 Hz frequency range, which contains the microseismic frequencies.

Due to experimental design such as station spacing, array linearity, and to the need for site permission from land owners/managers little leeway in station placement was afforded. Hence cultural effects contribute greatly to the variability in the higher frequencies. The sites most isolated from such activity show up well in the 1.0 -10 Hz range as dark blue in the ratio plots (Figure 7)

The Great Plains stations, comprised of TX01 - NM13, are located in and around oil/gas fields, significant agricultural activity, and urban areas. Figure 7 reveals higher noise levels at these sites relative to the overall array average levels. High frequency noise levels at stations NM14 - NM27 are lower, to slightly higher than average. NM27 is very isolated from cultural activity. It is however located on the eastern margin of the Rio Grande Rift. The other Rift stations (NM28 - NM33) show very high noise levels in the 1.0 - 10 Hz range. These sites are located in the relatively densely populated Rio Grande basin and transportation corridor. Sensors at these sites are placed on loose, unconsolidated fill material, which combined with the high amount of cultural activity may contribute to the higher than average noise levels seen in the higher frequencies.

Stations NM34 - UT54 span the Colorado Plateau. The majority of these stations are located on the Navajo Nation. Some of these sites were placed, for convenience and due to design restrictions, close to paved roads. NM37 - AZ47 are all fairly close to small towns along US highway

666 and other paved roads (highways) on the Navajo Reservation, resulting in the relatively higher than average high frequency noise levels observed at these stations.

In the higher frequencies the quietest span of stations in the RISTRA array lies between AZ48 and UT54, which are well within the Colorado Plateau as well as being the most remote sites.

High frequency SBN at MB04 is among the highest levels in the array. An interesting comparison can be made between stations MB04 and MB04b. Both stations were located in the Rio Grande Rift above the mid-crustal Socorro magma body. MB04 was located on loose soil outside of the PASSCAL instrument center on the grounds of the New Mexico Institute of Mining and Technology. It was moved during the course of the experiment to a new location (MB04b) on a concrete pier placed on bedrock at the entrance of a tunnel, about 2 miles from its original site. The difference in noise levels between the two is remarkable in that MB04 is among the noisiest sites in the array and MB04b is among the quietest. The difference in noise levels can be attributed to the differences in site and vault conditions. Also note in figure 7 as well as in the individual station plots in the appendix (Figure 9) that the long-period noise levels on the north-component are higher than those on the east-component, suggesting anisotropy.

On average long-period (0.003 -0.03 Hz) noise levels are higher on the two horizontal components than on the vertical (Figure 5). However the variability in long-period noise on the Z-components is greater than on the horizontal components (Figure A2). Tilt due to settling of the concrete pad in the vault may be responsible for some of the long-period noise. Interestingly, the mean long-period noise levels of the array are higher during the night time than the day on all three components. This may be due to temperature and pressure changes.

The Great Plains stations show relatively low, long-period noise levels -- except for NM13 which is the northwestern-most of the Plains stations. It has very high long-period noise levels of unknown origin.

Rift stations NM27 and NM28 have widely different site conditions, yet both have relatively high long-period noise levels. NM27 is located on bed rock some 400 m in elevation higher than NM28 on the eastern margin of the Rio Grande Rift. NM28 is located in the middle of the rift valley on loose sand, among the highest levels of cultural activity in the array.

The variability in the SBN levels across all frequencies along the RISTRA array most likely are due to variations in the individual site conditions.

References

- Given, H. K. (1990). Variations in broadband seismic noise at IRIS/IDA stations in the USSR with implications for event detection, *Bull. Seism. Soc. Am.* **80**, 2072-2088.
- Given, H. K., and J. F. Fels (1993). Site characteristics and ambient ground noise at IRIS/IDA stations AAK (Ala-archa, Kyrgyzstan) and TLY (Talaya, Russia), *Bull. Seism. Soc. Am.* **83**, 945-953.
- Gurrola, H., J. B. Minster, H. Given, F. Vernon, J. Berger, and R. Aster (1990). Analysis of high-frequency seismic noise in the western United States and eastern Kazakhstan, *Bull. Seism. Soc. Am.* **80**, 951-970.
- Li, Y., W. Prothero Jr., C. Thurber, and R. Butler (1994). Observations of ambient noise and signal coherency on the island of Hawaii for teleseismic studies, *Bull. Seism. Soc. Am.* **84**, 1229-1242.
- Peterson, J. (1993). Observations and modeling of seismic background noise, Open-File Report 93-322, U.S. Department of Interior Geological Survey.

- Powell, C. A. (1992). Seismic noise in northcentral North Carolina, *Bull. Seism. Soc. Am.* **82**, 1889-1909.
- Rodgers, P. W., S. R. Taylor, and K. K. Nakanishi (1987). System and site noise in the regional seismic test network from 0.1 to 20 Hz, *Bull. Seism. Soc. Am.* **77**, 663-678.
- Stutzmann, E., G. Roult, and L. Astiz (2000). GEOSCOPE station noise levels, *Bull. Seism. Soc. Am.* **90**, 690-701.
- Vila, J. (1998). The broadband seismic station CAD (Tunel del Cadi, eastern Pyrenees): Site characteristics and background noise, *Bull. Seism. Soc. Am.* **88**, 297-303.
- Withers, M. M., R. C. Aster, C. J. Young, and E.P. Chael (1996). High-frequency analysis of seismic background noise as a function of wind speed and shallow depth, *Bull. Seism. Soc. Am.* **86**, 1507-1515.
- Young, C. J., E. P. Chael, M. M. Withers, and R. C. Aster (1996). A comparison of high-frequency (>1 Hz) surface and subsurface noise environment at three sites in the United States, *Bull. Seism. Soc. Am.* **86**, 1516-1528.

Appendix

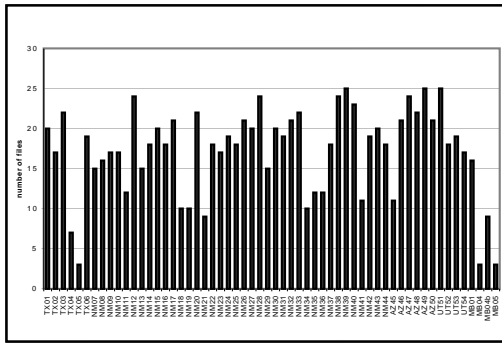
Table 1: RISTRA station locations

TABLE 1.

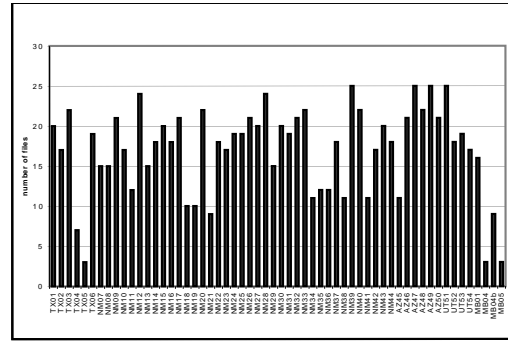
station	latitude/ longitude	elevation (m)	station	latitude/ longitude	elevation (m)
TX01	31.42324 -103.10536	750	NM30	34.74281 -106.97360	1515
TX02	31.51328 -103.10536	765	NM31	34.84911 -107.09767	1676
TX03	31.62320 -103.32361	831	NM32	34.98072 -107.26429	1685
TX04	31.73379 -103.4457	833	NM33	35.11066 -107.42286	2094
TX05	31.87845 -103.60737	873	NM34	35.26884 -107.64317	2735
TX06	31.96710 -103.70684	899	NM35	35.34481 -107.70697	2133
NM07	32.08454 -103.83999	966	NM36	35.44526 -107.82246	2176
NM08	32.19915 -103.97210	886	NM37	35.57755 -108.00173	2254
NM09	32.32648 -104.11830	893	NM38	35.70233 -108.16292	2077
NM10	32.47293 -104.26722	929	NM39	35.7926 -108.26736	1949
NM11	32.58364 -104.40850	974	NM40	35.94505 -108.42896	1796
NM12	32.68287 -104.50832	1066	NM41	36.03528 -108.57034	1718
NM13	32.80279 -104.65484	1177	NM42	36.14851 -108.71712	1794
NM14	32.90685 -104.75940	1219	NM43	36.24956 -108.88712	1991

TABLE 1.

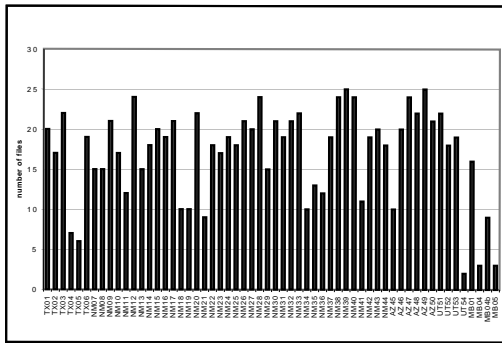
station	latitude/ longitude	elevation (m)	station	latitude/ longitude	elevation (m)
NM15	33.01441 -104.90936	1342	NM44	36.42138 -108.95827	1921
NM16	33.17406 -105.12670	1625	AZ45	36.45520 -109.08242	2683
NM17	33.25657 -105.17344	1705	AZ46	36.55126 -109.22942	2009
NM18	33.40295 -105.34096	1624	AZ47	36.63598 -109.33321	1752
NM19	33.49127 -105.45537	2028	AZ48	36.76064 -109.53932	1664
NM20	33.60478 -105.59350	2034	AZ49	36.8869 -109.69135	1512
NM21	33.73280 -105.74460	2000	AZ50	36.97769 -109.86372	1469
NM22	33.84036 -105.86888	1691	UT51	37.07315 -109.99605	1498
NM23	33.95027 -106.01240	1813	UT52	37.23478 -110.13132	1671
NM24	34.04687 -106.11961	1874	UT53	37.34585 -110.33107	1291
NM25	34.16698 -106.26052	1933	UT54	37.41870 -110.50516	1439
NM26	34.26328 -106.36329	1854	MB01	33.33631 -106.03395	1446
NM27	34.38562 -106.52386	1870	MB04	34.07384 -106.92015	1414
NM28	34.54034 -106.7002	1484	MB04b	34.07091 -106.94225	1489
NM29	34.64724 -106.84912	1561	MB05	34.66361 -108.01137	2143



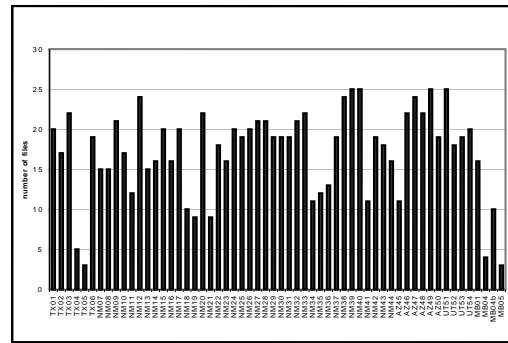
(a)



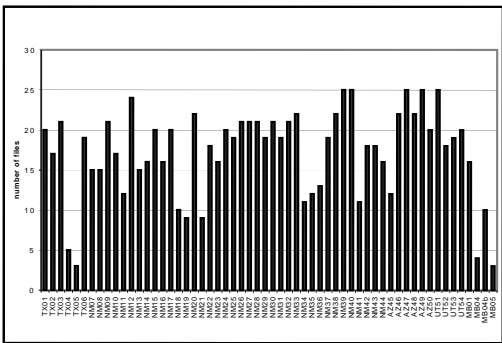
(b)



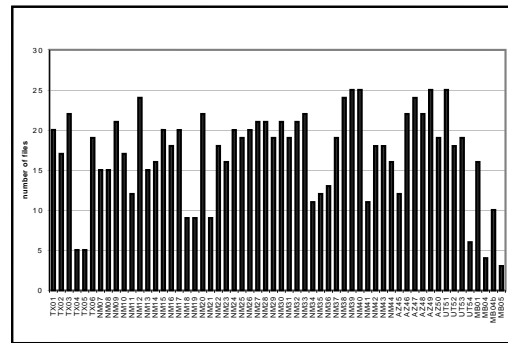
(c)



(d)



(e)



(f)

Figure A1. Number of files used in calculating station average PSD's. (a) "noisy" period east-component (b) "noisy" period north-component (c) "noisy" period vertical-component (d) "quiet" period east-component (e) "quiet" period north-component (f) "quiet" period vertical-component

